Journal of Materials Chemistry A

PAPER

View Article Online
View Journal | View Issue

Check for updates

Cite this: J. Mater. Chem. A, 2019, 7, 15207

A self-healing elastomer based on an intrinsic non-covalent cross-linking mechanism†

Jun Chen,‡[a] Fanzhu Li,‡[b] Yanlong Luo,‡[a] Yijun Shi,[c] Xiaofeng Ma,[a] Meng Zhang,[d] D. W. Boukhvalov[a] and Zhenyang Luo*[a]

Synthesis and comprehensive examination of a polyurethane (urea) elastomer that self-heals based on intrinsic dynamic non-covalent bonds (van der Waals and hydrogen) are reported. The dynamic non-covalent bonds include hydrogen bonds and van der Waals forces. The difference in the previous approach in which hydrogen bond self-healing materials introduced dense quadruple hydrogen bonds at the ends or branched chains poly(propylene carbonate) (PPC) diol was used as the soft segment of the polyurethane (urea) material, and strong van der Waals forces were provided by the large number of carbonyl groups in its main chain; hydrogen bonds were formed by urethane bonds, urea bonds, and the carbonyl groups on PPC. The mechanical properties and healing efficiency of the self-healing polyurethane (urea) elastomer were studied. *In situ* temperature-dependent infrared and low-field nuclear magnetic resonance (LNMR) measurements were combined with molecular dynamics simulations to investigate the self-healing mechanisms. The results of the studies on the self-healing polyurethane demonstrate that the dynamic cross-linking between hydrogen bonds and van der Waals forces is the basic driving force for the self-healing ability of the material, and temperature is the key factor that affects hydrogen bonding and van der Waals forces. The effect of crystallization on the self-healing ability of the material was also studied. The molecular dynamics simulation results also demonstrate interplay between van der Waals forces and hydrogen bonds at different temperatures.

Received 10th April 2019
Accepted 29th May 2019

DOI: 10.1039/c9ta03775f

rsc.li/materials-a

Published on 29 May 2019. Downloaded on 12/9/2019 6:16:24 AM.

Introduction

The development of self-healing materials not only significantly improves the safety and efficiency of materials, but also reduces energy consumption and achieves social sustainability. The advantage of organic polymer materials is that the structure can be freely regulated, which has attracted global research interest. There are two kinds of covalent bonds: dynamic covalent bonds and dynamic non-covalent bonds, and among them the dynamic covalent bonds are easy to achieve and show better self-healing performance. So dynamic covalent bonds play a key role in the designing of self-healing materials.[1–6]

Fu *et al.* used the Diels–Alder reaction as the main mechanism to synthesize a polyurethane matrix with a furan ring at the end and they further made a hyperbranched polymer HSiNCM, using KH560 and NCM. In addition, a PU–DA–CNT material was obtained by adding oxidized carbon nanotubes, aCNTs, in which the silane acted as a chemical cross-linker, while carbon nanotubes and amide bonds acted as physical cross-linkers. Combined with a DA reversible reaction, a triple three-dimensional dynamic cross-linking network was constructed to achieve self-healing properties.[3] Similarly, Fang *et al.* modified a hydroxyl position of the 2-hydroxyanthracene ring with acryloyl chloride based on the reversible cross-linking of the anthracene ring, which reacted with diethanolamine to provide an anthracene derivative containing hydroxyl groups. The hydroxyl modified anthracene ring was used as a chain extender to obtain a self-healing polyurethane material with photothermal response. However, special external conditions were required for these reversible covalent self-healing materials.[7]

Recently, researchers have studied a non-covalent reversible cross-linking mechanism to obtain self-healing materials without external stimuli. Chen *et al.* prepared a polyurethane material *via* stepwise polymerization of methyl diethanolamine (MDEA) and hexamethylene isocyanate (HDI), where the nitrogen atoms of MDEA were used as the core to introduce 1,3-propanesultone. The S–C bonds broke and N^+ ions formed from N eventually resulting in a polyurethane material with a dynamic cross-linked network through static electricity.[8] Wang *et al.* reported a HBN-GO elastomer based on graphene oxide and HB-NH_2, where the amide bond was prepared by the

[a]College of Science, Nanjing Forestry University, 159 Longpan Road, Nanjing 210037, P. R. China. E-mail: luozhenyang@njfu.edu.cn
[b]Key Lab Beijing City Preparat & Proc Novel Polyme, State Key Lab Organ Inorgan Composites, Beijing University of Chemical Technology, Beijing, 100029, P. R. China
[c]Division of Machine Elements, Luleå University of Technology, 97187 Luleå, Sweden
[d]Institute of Chemical Industry of Forestry Products, CAF, Nanjing, 210042, P. R. China

† Electronic supplementary information (ESI) available. See DOI: 10.1039/c9ta03775f

‡ J. Chen, F. Li and Y. Luo equally contributed to this paper.

Published on 29 May 2019. Downloaded on 12/9/2019 6:16:24 AM.

reaction between macromolecular tricarboxylic acids and amino groups, and the graphene oxide was then mixed to achieve physical and chemical cross-links.[9]

Other researchers have introduced chemical bonds with reversible functions in the main chain to further reduce the complexity during synthesis, and obtain high strength self-healing polyurethane at the same time. Kim's group prepared high-strength self-healing polyurethane materials with a polyether diol and chain extenders containing disulfide bonds. The isocyanates, including aromatic and aliphatic isocyanates, were investigated, and the samples with IPDI as the hard segment had the highest healing efficiency and the best performance.[10] Lin *et al.* synthesized a polyurethane using IPDI and PEG-2000 as raw materials, where the end was terminated with SCMHBMA. A self-healing polyurethane material based on hydrogen bonding resulting from the dense hydrogen bonds at the end of the main chain was obtained.[5] In this work, they introduced a group containing hydrogen bonds at the end of the polyurethane molecular chain, which is a complicated process and does not fully utilize the structural characteristics of the macromolecular chain.

In addition to experimental methods, molecular dynamics simulation has also been proved to be an effective means to study the self-healing behaviour and mechanism of materials. For example, Sun *et al.* simulated the sensitive self-healing characteristics of asphalt adhesives based on molecular dynamics, and by simulating the motion trajectory of two parts of asphalt molecules and the distribution of relative concentration in the *o–z* direction, they could explain the mechanism of self-healing by molecular simulation. These simulations provide a molecular basis for the healing behaviour and mechanism of materials.[11]

Few studies on the self-healing mechanism of hydrogen bonding and van der Waals forces are reported. Many researchers reported high-strength materials by using dynamic covalent bonding as the main mechanism of the healing process, which faces some problems, such as materials toxicity, complex synthetic processes, and being economically costly and difficult to industrialize. In addition, dynamic covalent bonds are generally sensitive to the external conditions, such as light, heat, *etc.* In order to overcome the above problems, this paper focuses on the designing of self-healing materials based on intrinsic non-covalent interactions in combination with the solidification of carbon dioxide. Blattmann's group pointed out that carbon dioxide as a source of polyurethane can give better performance and more functions in future research, and will replace traditional polyurethane. The development of a new healing mechanism will provide new directions and applications for polycarbonate polyurethane materials.[12]

A few studies on the intrinsic dynamic non-covalent healing mechanism are reported in the literature. Takuzo Aida has recently reported a self-healing thiourea polymer based on the intrinsic hydrogen bonding mechanism, where the hydrogen bonds with unequal lengths in thiourea were used to reduce the crystallinity of the material, and a rheometer combined with theoretical calculations was used to investigate the effects of different types of molecular chains on the dynamic bonding of hydrogen bonds in thiourea.[13] Similarly, Urban *et al.* also reported a commodity copolymer with an intrinsic non-covalent self-healing ability. Combined with molecular simulations, they found that the molecular chain could form a special key–lock structure under the action of van der Waals forces when the molar ratios of methyl methacrylate to *n*-butyl acrylate were between 30/70 and 70/30 and achieved a self-healing ability of 90–100%.[14] These reports have played a guiding role in the development of self-healing materials *via* intrinsic dynamic non-covalent interactions. The research on dynamic covalent bonds is like a hundred flowers in bloom, and the research on dynamic non-covalent bonds is still rare.

On the basis of the above reports, propylene polycarbonate was obtained by the copolymerization of carbon dioxide and propylene oxide in a molar mass ratio of 3 : 4, but their characteristic properties have not been explored.[15,16] Here we designed PPC–PU with high cohesive energy, strong van der Waals forces, and good flexibility due to the alternating carbonyl and ether bonds, and the activity of the soft segment of the molecular chain was maintained at room temperature. We also found that the dynamic physical cross-linking of the material could be attributed to van der Waals forces and hydrogen bonds on the main chain using PPC as hydrogen bond acceptors (carbonyl) and hydrogen bond donors (active hydrogen) introduced by urethane bonds and urea bonds.

In this study, a self-healing polyurethane material was synthesized by skilfully selecting the soft and hard segments of the appropriate polyurethane, and the interaction between hydrogen bonding and van der Waals force (dynamic non-covalent cross-linking) is proposed as the healing mechanism by combining molecular dynamics simulation. This is a development of the existing research, and enriches the theory of the self-healing mechanism of intrinsic non-covalent bonds of polyurethane (urea). The polypropylene carbonate used here utilizes carbon dioxide as a raw material, and the facilitation on carbon dioxide recycling is remarkable. The isocyanate and chain extender can be replaced by the same type of product, and the synthetic process is simple, which is beneficial for industrial application in a wide range of polyurethanes, and provides a good theoretical basis for large-scale application of self-healing materials.

Experimental

Materials

Polypropylene carbonate polyol (PPC, $M_w = 3000 g\ mol^{-1}$) was purchased from Guangdong Dazhi Environmental Protection Technology Co., Ltd., China. 4,4′-Diphenyl methane diisocyanate (MDI) was obtained from Wanhua Chemical Group Co., Ltd., China. 1,6-Hexamethylenediamine and *N*′*N*-dimethylformamide (DMF) were bought from Shanghai Macklin biochemical Technology Co., Ltd. All the above chemicals were used as received.

Preparation of polyurethane materials

According to Table 1, PPC and MDI were mixed by stirring for 45 min at 80 °C, into which DMF was added. The chain extender

 This journal is © The Royal Society of Chemistry 2019

Published on 29 May 2019. Downloaded on 12/9/2019 6:16:24 AM.

1,6-hexamethylenediamine was added to the solution and maintained at 20 °C for 2 h to obtain a chain extension PU solution. The solvent was dried to obtain polyurethane (urea).

Conditions of characterization

The complete spline was cut with a scalpel, and the sections were spliced and kept at different temperatures for 2 h. The sample of polyurethane is a dumbbell spline: the total length is 100 mm, the standard width is 10 mm, the standard length is 6 mm, and the thickness is 1 mm. The tensile rate is 10 mm min^{-1}. The strength of the polyurethane was recorded with a tensile testing machine (CMT4204 SANS, China).[17] *In situ* FTIR spectra were obtained using a micro-infrared coupled rheometer (Thermo Fisher MAS60, Germany) at different temperatures. The test range was 4000 cm^{-1}–500 cm^{-1}, the resolution was 4 cm^{-1}, and the number of scans was 16. The temperature range was 25–95 °C. ^{1}H-LNMR spectra were recorded on a Low-field Nuclear Magnetic Resonance (LNMR) (Numag VTMR20-010-T 20 M, China) instrument at different temperatures; the temperature range was 25–75 °C.

Modeling and simulation details

In the simulation process, 3d periodic boundary conditions are used (Fig. 1). Initially, the smart minimizer method was used to minimize the energy of the 3d periodic cell, and the standard of energy convergence was 1.0×10^{-5} kcal mol^{-1} $Å^{-1}$. The periodic boundary conditions can be observed by building a supercell with 9 representative volume elements (3 by 3), as shown in Fig. S1.† And then, in a vacuum we simulated five cycles of annealing at the temperature range of 300–500 K with 10 gradients to cool down at each loop. The goal of the energy minimization and annealing simulations was to obtain sufficiently relaxed molecular chain conformations. Finally, 1000 ps of NVT (constant atoms, volume, and temperature) annealing was simulated with a system of 1000 ps and one atmospheric pressure, and a system simulation of NPT (constant atomic number, pressure and temperature). In order to study the effect of temperature on the system, the simulation temperatures used were 25 °C, 50 °C and 75 °C and the initial density was 1.0 g cm^{-3}. A Berendsen pressure regulator was used to control the pressure and a thermostat was used for temperature control. Calculations of electrostatic interaction (Eelec) and van der Waals interactions (EvdW) were performed using the Ewald method and the Lennard-Jones function, respectively, in non-key energy calculations. The accuracy of the Ewald method was 0.001 kcal mol^{-1}, and the truncation radius of the Lennard-Jones function was 12.5 Å. Using the Verlet velocity integral method to integrate Newton's equations, the integral step was 1 fs. The simulation software was Materials Studio, and the force field was COMPASS (Condensed-Phase Optimized Molecular Potentials for Atomistic Simulation Studies).[18–21]

Table 1 Formula of the PU

Formula	PPC/mol	MDI/mol	1,6-Hexane diamine/mol
1#PU	1	1.2	0.2
2#PU	1	1.4	0.4
3#PU	1	1.6	0.6
4#PU	1	1.8	0.8
5#PU	1	2	1

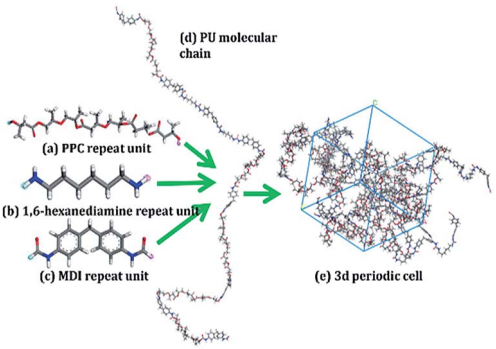


Fig. 1 Simulated unit and cell construction process (gray balls, red balls, blue balls and white balls represent carbon atoms, oxygen atoms, nitrogen atoms and hydrogen atoms, respectively).

Results and discussion

To facilitate two non-covalent bonds in the polyurethane (urea) material, a highly polar PPC diol was added to the material to provide sufficiently strong van der Waals forces. The urethane bonds and the urea bonds were formed using an amine chain extender and were used to introduce dispersed hydrogen bonding groups. The carbonyl groups on the PPC also formed hydrogen bonds with the urethane bonds and the urea bonds in addition to the strong van der Waals forces.[22] These were combined with the hydrogen bonds between the urethane bonds and the urea bonds constituting a reversible non-covalent bond network to realize the self-healing ability of the polyurethane (urea). The following characterization methods were used to test this mechanism.

Self-healing efficiency of the poly(propylene carbonate)–polyurethane (urea) elastomer (PPC–PU)

The tensile strength of the material increased with increasing isocyanate content (Fig. 2), because of the increase in crystallinity. Therefore, sample #5 could not be tested for mechanical properties after healing because its healing efficiency decreased to 0%. Sample #1 could not be tested for mechanical properties because of its low strength, and had low crystallinity. All samples had various degrees of self-healing ability. The PU of different formulae had the highest healing efficiency at 50 °C. The healing strength of PU #3 could reach the initial strength, and the healing efficiency could reach 100%. At 75 °C, the healing efficiencies were slightly lower than those at 50 °C, but higher than the initial values at 25 °C.

Table 2 shows that 50 °C was the best healing temperature. The elongation at break of the material decreased after healing. This is because the material had a large number of covalent

Published on 29 May 2019. Downloaded on 12/9/2019 6:16:24 AM.

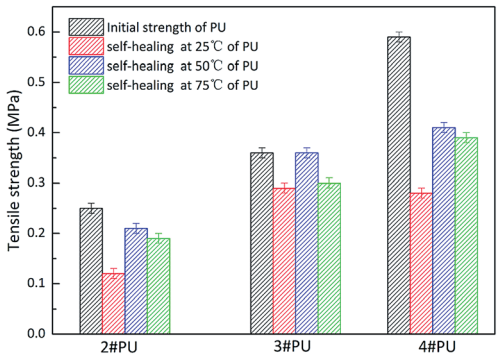


Fig. 2 The initial strength of polyurethane and the strength after repairing at different temperatures.

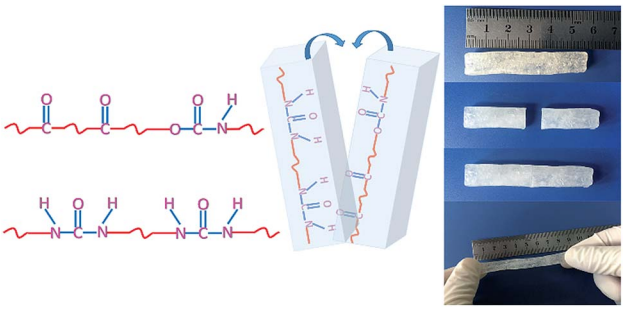


Fig. 3 Schematic diagram of the self-healing mechanism.

bonds destroyed in addition to non-covalent bonds. Since the healing ability relies on the recombination of a large number of hydrogen bonds and van der Waals forces, and the molecular chain on the fracture surface did not have full diffusion, the elongation at break of the material could not be fully recovered.[23]

We proposed that the recombination of hydrogen bonds *via* van der Waals forces is the main healing mechanism as shown in Fig. 3. To examine the discussed self-healing mechanism, the materials were tested *via in situ* infrared spectroscopy and LNMR, which were combined with molecular dynamics simulation to calculate the hydrogen bonding forces and van der Waals forces. The final calculated results were consistent with the experimental results as described below.

Infrared spectra of hydrogen bonds of PPC–PU

Hydrogen bonds are weaker than conventional polar bonds but stronger than van der Waals forces. The maximum hydrogen bond principle indicates that hydrogen bonds in polymer materials are always formed as much as possible. The absorption bands associated with the stretching vibrations of the N–H bonds were red-shifted, widened, or strengthened due to the formation of hydrogen bonds.[24–28] This phenomenon is reflected in Fig. 4(a) and (b). The absorption peak of the stretching vibration of the N–H bonds was red-shifted when the temperature was increased from 25 °C to 55 °C with an increase in the absorption intensity, while a blue shift occurred when the temperature increased from 55 °C to 95 °C with decreased intensity. The maximum absorption peak intensity was observed at 55 °C.

Fig. 4(c) and (d) show that the absorption band position and the peak intensity of the C=O bonds changed with temperature, and the maximum red shift and peak intensity were also observed at 55 °C. This phenomenon indicated that hydrogen bonds were formed inside the material at 25 °C to 55 °C. The formation of hydrogen bonds caused the peaks of the amino groups and the carbonyl groups to shift to low wavenumbers with an increase in the peak intensities. The hydrogen bonds separated from 55 °C to 95 °C causing the peaks of the amino groups and the carbonyl groups to shift to high wavenumbers with a decrease in peak intensities. This phenomenon indicated that the urethane bonds, the urea bonds, and the carbonyl groups on PPC were all involved in the formation and dissociation of hydrogen bonds. The hydrogen bonds were affected by temperature, which affected the self-healing efficiency of the material.[13,14,24]

Fig. 5 shows the relationship between the areas of infrared absorption peaks of the amino groups and carbonyl groups and temperature as well as the first-order differential. The areas of the absorption peaks decreased with increasing temperature, but the variation rates were very different between the amino groups and the carbonyl groups. The areas of the absorption peaks of the amino groups varied with temperature, and transition points appeared at 41 °C and 85 °C; correspondingly, the transition points for the areas of the absorption peaks of the carbonyl groups were observed at 45 °C and 78 °C.

Fig. 4 shows the transition point of the red-shift of the amino groups and the blue shift of the carbonyl groups at 55 °C obtained *via in situ* infrared spectroscopy. There were overlapping regions of the two peaks in the differential curve. The hydrogen bonds were continuously formed during the temperature rise, and the hydrogen bonds were the strongest when the first temperature transition zone (41–45 °C) was reached. The hydrogen bonds were substantially dissociated when the temperature reached the second transition zone (78–85 °C). In these two temperature transition zones, the formation rate of the hydrogen bonds was higher than the dissociation rate;

Table 2 Mechanical properties of polyurethane before and after self-healing

	2#PU				3#PU				4#PU			
Condition	Initial	25 °C	50 °C	75 °C	Initial	25 °C	50 °C	75 °C	Initial	25 °C	50 °C	75 °C
Elongation at break/%	90.29	50.32	76.84	69.23	80.81	22.62	49.67	18.50	71.04	24.99	34.3	51.37
Repair efficiency/%		44	78	70		80	100	83		47	69	66

This journal is © The Royal Society of Chemistry 2019

Published on 29 May 2019. Downloaded on 12/9/2019 6:16:24 AM.

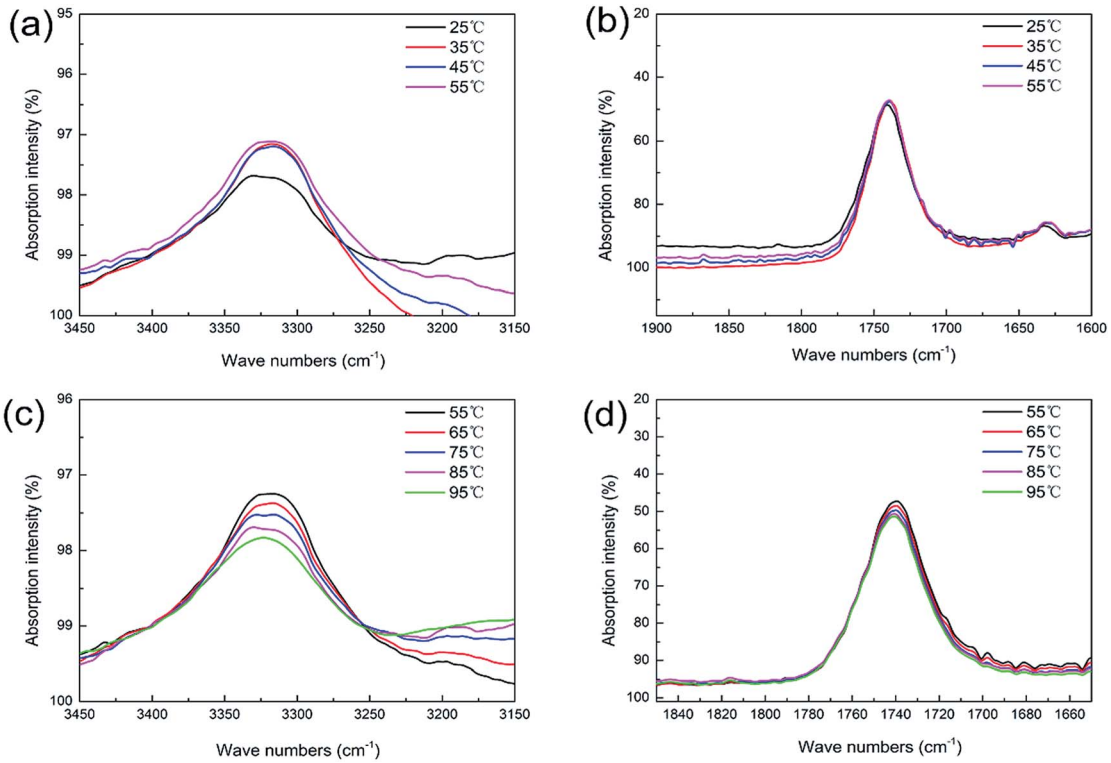


Fig. 4 *In situ* temperature swing infrared spectra of 3#PU: (a) amino, 25–55 °C; (b) carbonyl, 25–55 °C; (c) amino, 55–95 °C; (d) carbonyl, 55–95 °C.

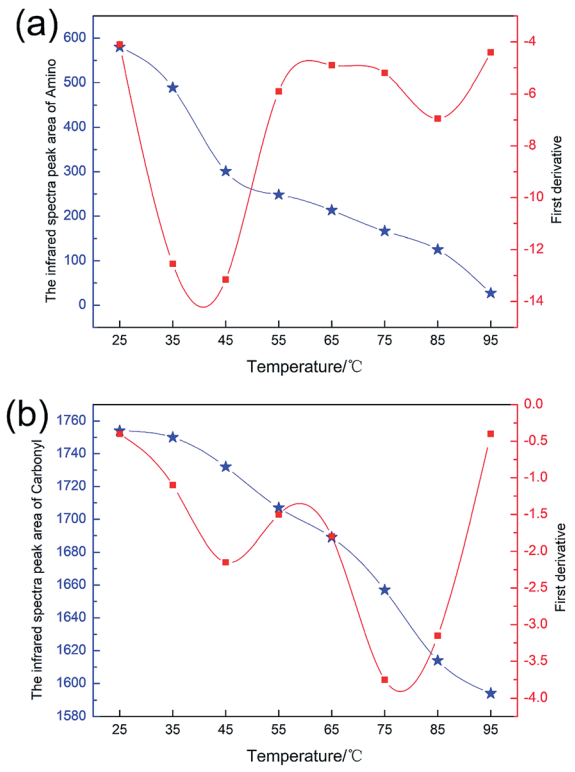


Fig. 5 Peak areas of infrared spectra with temperature variation and the first derivative: (a) amino and (b) carbonyl.

however, this gradually transitioned into a state where the formation rate was lower than the dissociation rate, and the hydrogen bonds were in a dynamic binding state. The temperature trend reflected in the infrared spectra was consistent with the macroscopic phenomenon of self-healing of the polyurethane (urea) material. By comparing with Fig. 2, we concluded that the polyurethane (urea) material has enhanced movement of the main chain when the appropriate temperature range was reached. This is beneficial to the formation of hydrogen bonds. A high self-healing efficiency was achieved, which showed that the hydrogen bonds were some of the key factors in the self-healing of the polyurethane (urea) material.

Low-field nuclear magnetic resonance of the hydrogen bonds of PPC–PU

LNMR, also known as time-domain NMR, can specifically study molecular motion characteristics. It can detect the relaxation time of hydrogen protons. The relaxation time of hydrogen protons varied for different materials and different chemical environments. Inside the polymer elastomer, in addition to the constraint of C–H bonds on hydrogen protons, hydrogen bonds and van der Waals forces were also constrained in hydrogen protons. Both hydrogen bonds and strong van der Waals forces can decrease the degree of freedom of hydrogen protons and the relaxation time.[29,30] Therefore, hydrogen bonds can be investigated by analysing the change in the relaxation time of hydrogen protons in the polyurethane (urea) material.

Published on 29 May 2019. Downloaded on 12/9/2019 6:16:24 AM.

Sample #3 has the highest self-healing efficiency, and we analyzed the change in the relaxation time of hydrogen protons in sample #3 at different temperatures. The bond energy of the C–H bonds is higher than that of the N–H bonds. Therefore, the relaxation time of the hydrogen protons in the C–H bonds was shorter than that of the hydrogen protons in the N–H bonds. Fig. 6 shows that the peak with a shorter relaxation time corresponded to the hydrogen protons of the C–H bonds in the PPC–PU material. The peak with a long relaxation time corresponded to the hydrogen protons in the N–H bonds. As the temperature increased, the van der Waals forces weakened, and the constraint to the hydrogen protons in the C–H bonds weakened. This resulted in a continuous increase in the relaxation time. The relaxation time of hydrogen protons in the N–H bonds shortened and then prolonged as the temperature increased.

The changes in the relaxation time of the hydrogen protons in the C–H bonds and N–H bonds shown in Fig. 6 were integrated into a molecular structure diagram (Fig. 7). Combining Fig. 6 and 7, we found that the relaxation time of the N–H bonds was 54 ms at 25 °C. This reduced to 20 ms at 50 °C, and the relaxation time increased to 43 ms at 75 °C. According to Fig. 4, the formation of hydrogen bonds led to a decrease in the relaxation time of hydrogen protons in the N–H bonds at 25 °C to 50 °C. Hydrogen bonds dissociated at 50 °C to 75 °C, and the relaxation time of hydrogen protons in the N–H bonds increased to the value closest to that in the initial state. However, the relaxation time did not fully recover indicating that the hydrogen protons in the N–H bonds were still bound by weak hydrogen bonds.

The activity of the polyurethane (urea) main chain was enhanced when the van der Waals forces decreased with increasing temperature. Although the hydrogen bonds formed at a lower temperature began to dissociate, there were still some hydrogen bonds remaining. Thus, the relaxation time was not fully recovered. The LNMR results further indicated that the formation and dissociation of hydrogen bonds occurred simultaneously between 25 °C and 75 °C; the hydrogen bonds were then in a dynamic and reversible state.

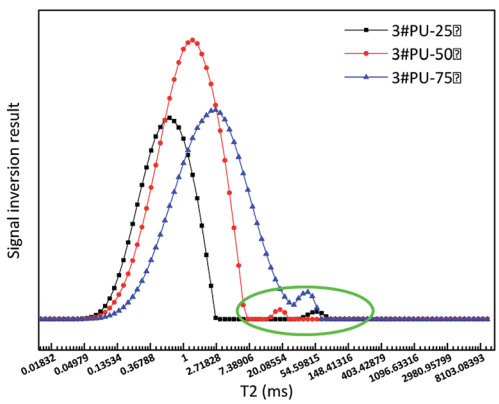


Fig. 6 Low-field nuclear magnetic resonance spectra of 3#PU.

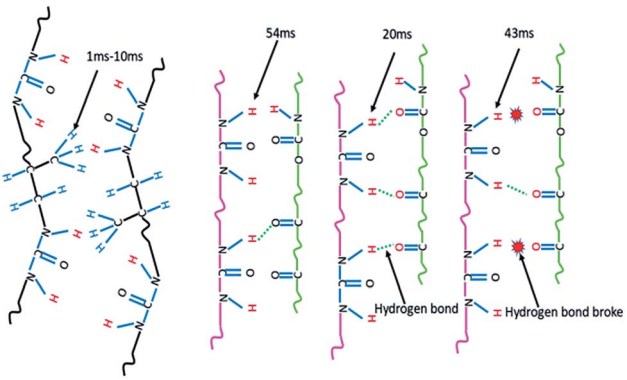


Fig. 7 Schematic diagram of hydrogen proton relaxation time in polyurethane (urea) materials.

Simulation of the change in hydrogen bonds and van der Waals forces in PPC–PU with temperature

MD simulation of sample #3 was performed at different temperatures (25 °C, 50 °C and 75 °C), and the results reveal that much more hydrogen bonds can be formed in the system (Fig. 8), and there are also van der Waals forces. The simulation results also demonstrate that hydrogen bonds were formed between the urethane bonds, the urea bonds and the carbonyl groups.

The density, cohesive energy density and intermolecular van der Waals forces of the system decreased with the increase of the temperature (Table 3). The negative values of van der Waals forces indicate that the molecules are attracted to each other, and the decrease of van der Waals interactions results in a prolonged relaxation time of hydrocarbon protons. The contribution of van der Waals interactions is larger than that of

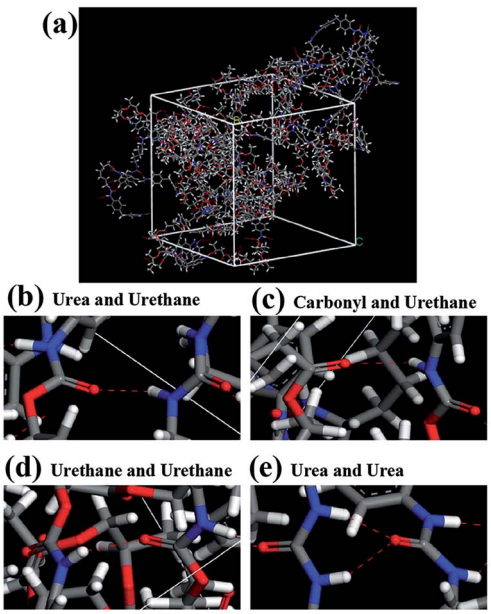


Fig. 8 Hydrogen bonds (b–e) in amorphous cells (a), (black dotted lines indicate 12 hydrogen bonds; gray, red, blue, and white bars represent carbon, oxygen, nitrogen, and hydrogen atoms, respectively).

This journal is © The Royal Society of Chemistry 2019

Published on 29 May 2019. Downloaded on 12/9/2019 6:16:24 AM.

Table 3 Energy and hydrogen bond number change with temperature for 3#PU

	Density (g cm^{-3})	CED (J cm^{-3})	E_{vdW} (kcal mol^{-1})	E_{elec} (kcal mol^{-1})	Number of H-bonds
25 °C	1.128	362.5	−1064.2	−340.4	49
50 °C	1.119	351.6	−1020.4	−379.6	60
70 °C	1.082	339.4	−994.0	−369.1	52

electrostatic interactions. Robust van der Waals interactions in the system can be attributed to the large amount of carbonyl groups on the PPC segment in the PU molecular chain, which indicates that van der Waals interaction also plays an important role in the self-healing process of PU.

The electrostatic interactions and the number of hydrogen bonds in the system increased first and then decreased with increasing temperature. The electrostatic interactions are the strongest at 50 °C, which corresponds with the increase in the number of hydrogen bonds, because the activity of polymer main chains was enhanced, more groups formed hydrogen bonds. Due to the increase of the hydrogen bonds the hydrogen proton relaxation time is minimum when the temperature is 50 °C; as temperature continues to rise, the hydrogen bonds begin to break and the hydrogen proton relaxation time increases again. The process of hydrogen bond breaking and regeneration is shown in Fig. 9. The simulated dynamic change of hydrogen bonds is consistent with the infrared spectra and LNMR test results, which proves that there is a dynamic exchange in the process of hydrogen bond healing, and the number of bonds and strength of the hydrogen bonds will be affected with the change of temperature.

The above simulation proves that the low-field NMR test results are correct. It also proves that from our in-depth analysis of the infrared spectrum, in the process of heating, hydrogen bond dissociation and formation occurs at the same time. The formation and dissociation rates are different at different temperature stages. The enhancement of hydrogen bonding makes up for the adverse effects caused by the van der Waals forces, so that the material can still achieve excellent healing efficiency.[18–21,31]

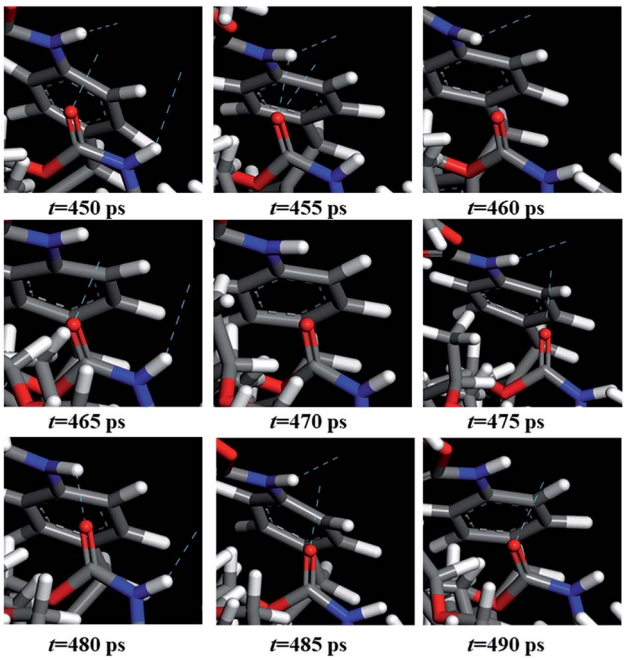


Fig. 9 Simulation of the hydrogen bond dynamic change process (blue dotted lines indicate hydrogen bonds; gray, red, blue, and white bars represent carbon, oxygen, nitrogen, and hydrogen atoms, respectively).

Conclusions

In this study, the dynamic cross-linking of intrinsic non-covalent bonds within the material was achieved through strong van der Waals forces introduced by the high carbonate content of PPC as well as the hydrogen bonds formed by the urethane bonds, the urea bonds, and the carbonyl groups in PPC. The self-healing ability of the polyurethane (urea) material under the dual action of van der Waals forces and hydrogen bonds was confirmed. These data and the molecular dynamics simulations showed that the non-covalent bonds inside the material were sensitive to temperature: the van der Waals forces decreased with increasing temperature while the hydrogen bonding first increased and then decreased with increasing temperature.

In summary, the amorphous PPC main chain reduced the rigidity of the macromolecular chain of polyurethane (urea) to produce large molecular segment movement. This resulted in the appearance of an array of nonlinear hydrogen bonds and introduced strong van der Waals forces to promote the interactions between molecular chains. The combination of these three actions activated the dynamic exchange of "hydrogen bonding pairs". These strongly interacting hydrogen bonds and van der Waals forces enabled the construction of multiple dynamic cross-linking networks based on non-covalent bonds leading to self-healing of the polyurethane (urea) elastomer.

Conflicts of interest

There are no conflicts to declare.

Acknowledgements

This work was supported by a project funded by the Priority Academic Program Development of Jiangsu Higher Education Institutions (PAPD). This work also was supported by the National Natural Science Foundation of China (31670578). The authors are grateful for the *in situ* infrared instruments and low-field nuclear magnetic instruments provided by the Advanced Analysis and Testing Center of Nanjing Forestry University, and the guidance of Ms Xiao fang Ma and Dr Yan Xuan.

Published on 29 May 2019. Downloaded on 12/9/2019 6:16:24 AM.

Notes and references

1 J. Leng, X. Lan, Y. Liu and S. Du, *Prog. Mater. Sci.*, 2011, **56**, 1077–1135.
2 Y. Chen, A. M. Kushner, G. A. Williams and Z. Guan, *Nat. Chem.*, 2012, **4**, 467–472.
3 A. Feula, A. Pethybridge, I. Giannakopoulos, X. Tang, A. Chippindale, C. R. Siviour, C. P. Buckley, I. W. Hamley and W. Hayes, *Macromolecules*, 2015, **48**, 6132–6141.
4 Z. Wang, C. Xie, C. Yu, G. Fei, Z. Wang and H. Xia, *Macromol. Rapid Commun.*, 2018, **39**, 1700678.
5 Y. Lin and G. Li, *J. Mater. Chem. B*, 2014, **2**, 6878–6885.
6 Y. Li, F. Gao, Z. Xue, Y. Luan, X. Yan, Z. Guo and Z. Wang, *Mater. Des.*, 2018, **137**, 438–445.
7 W. Fang, L. Liu, T. Li, Z. Dang, C. Qiao, J. Xu and Y. Wang, *Chem.–Eur. J.*, 2016, **22**, 878–883.
8 S. Chen, F. Mo, Y. Yang, F. J. Stadler, S. Chen, H. Yang and Z. Ge, *J. Mater. Chem. A*, 2015, **3**, 2924–2933.
9 C. Wang, N. Liu, R. Allen, J. B. H. Tok, Y. Wu, F. Zhang, Y. Chen and Z. Bao, *Adv. Mater.*, 2013, **25**, 5785.
10 S. Kim, H. Jeon, S. Shin, S. Park, J. Jegal, S. Y. Hwang, D. X. Oh and J. Park, *Adv. Mater.*, 2018, 30.
11 D. Sun, G. Sun, X. Zhu, F. Ye and J. Xu, *Fuel*, 2018, **211**, 609–620.
12 H. Blattmann, M. Fleischer, M. Baehr and R. Muelhaupt, *Macromol. Rapid Commun.*, 2014, **35**, 1238–1254.
13 Y. Yanagisawa, Y. Nan, K. Okuro and T. Aida, *Science*, 2018, **359**, 72.
14 M. W. Urban, D. Davydovich, Y. Yang, T. Demir, Y. Zhang and L. Casabianca, *Science*, 2018, **362**, 220.
15 S. Si, B. Liu, C. Liu, T. Yang and Z. Feng, *Chin. J. Geophys.*, 2017, **60**, 999–1006.
16 X. Li, Y. Pei, B. Liu, Y. Zhao, C. Liu, Q. Xie, Q. Hua and S. Deng, *Chin. J. Geophys.*, 2009, **52**, 2291–2301.
17 Y. Heo, M. H. Malakooti and H. A. Sodano, *J. Mater. Chem. A*, 2016, **4**, 17403–17411.
18 D. Sun, G. Sun, X. Zhu, Q. Pang, F. Yu and T. Lin, *Constr. Build. Mater.*, 2017, **132**, 230–239.
19 H. Wan, J. Shen, N. Gao, J. Liu, Y. Gao and L. Zhang, *Soft Matter*, 2018, **14**, 2379–2390.
20 Y. Huang, P. Chuang and C. Chen, *Int. J. Heat Mass Transfer*, 2015, **91**, 45–51.
21 S. Y. Kim, H. G. Jang, C. Yang and B. J. Yang, *Compos. Sci. Technol.*, 2018, **155**, 169–176.
22 Y. Song, Y. Liu, T. Qi and G. L. Li, *Angew. Chem., Int. Ed.*, 2018, **57**, 13838–13842.
23 Y. Zhang, G. Yang, Y. Wang, X. Lu, G. Wu, Z. Zhang, K. Wang, R. Zhang, P. F. Nealey, D. J. Darensbourg and Z. Xu, *Macromolecules*, 2018, **51**, 791–800.
24 S. Lei, K. Tahara, F. C. De Schryver, M. Van der Auweraer, Y. Tobe and S. De Feyter, *Angew. Chem., Int. Ed.*, 2008, **47**, 2964–2968.
25 M. J. Minch, *J. Chem. Educ.*, 1999, **76**, 759.
26 C. Aakeroy, *Cryst. Growth Des.*, 2001, **1**, 255.
27 M. K. Krepps, S. Parkin and D. A. Atwood, *Cryst. Growth Des.*, 2001, **1**, 291–297.
28 G. C. Pjmentel and A. L. Mcclellan, *Annu. Rev. Phys. Chem.*, 1971, **22**, 347–385.
29 W. Jiang, S. Yang, X. Sun, W. Lu, D. Jiang, L. Xu, H. Xu, B. Gao, M. Ma and F. Cao, *Anal. Methods*, 2018, **10**, 2494–2502.
30 Y. Zhao, Y. Yao, M. Xiao, Y. Chen, C. C. C. Lee, L. Zhang, K. X. Zhang, S. Yang and M. Gu, *Food Control*, 2013, **34**, 436–443.
31 D. Sun, G. Sun, X. Zhu, F. Ye and J. Xu, *Fuel*, 2018, **211**, 609–620.

This journal is © The Royal Society of Chemistry 2019